Electronic Supplementary Information

A versatile and accessible polymer coating for functionalizable zwitterionic quantum dots with high DNA grafting efficiency

Chloé Grazon,[a,b,§] Margaret Chern,[c,§] Katherine Ward,[d] Sébastien Lecommandoux,[a] Mark W. Grinstaff,[b,d] and Allison M. Dennis[c,d,*]

a. Univ. Bordeaux, CNRS, Bordeaux INP, LCPO, UMR 5629, F-33600, Pessac, France.
b. Department of Chemistry, Boston University, Boston, MA, USA
c. Division of Materials Science and Engineering, Boston University, Boston, MA, USA
d. Department of Biomedical Engineering, Boston University, Boston, MA, USA
§ These authors contributed equally.
* Email: aldennis@bu.edu

Experimental details

MATERIALS

Poly(isobutylene-*alt*-maleic anhydride) (PIMA – 6,000g/mol), (2-aminoethyl)trimethylammonium chloride (Me_3N^+-NH_2), histamine (his), triethylamine, 4-(2-hydroxyethyl)-1-piperazineethanesulfonic acid (HEPES), sodium bicarbonate ($NaHCO_3$), agarose, and streptavidin-coated agarose beads were obtained from Sigma-Aldrich. mPEG-NH_2 (550 g/mol) is from LaysanBio. Dibenzocyclooctyne-amine (DBCO-NH_2) was bought from Click Chemistry Tools. SYBR™ Green I Nucleic Acid Gel Stain (10,000x concentrate in DMSO) and 10x TAE (Tris-Acetate-EDTA) buffer were bought from ThermoFisher Scientific. Oligonucleotides were purchased from IDT Technologies. HPLC-grade solvents including hexanes (Fisher Scientific), methanol (Honeywell), anhydrous dimethyl sulfoxide (DMSO; Sigma Aldrich) and chloroform (J.T. Baker) were used without further purification. Sulfobetaine-amine (Zw, Scheme S1) was synthesized according to literature.[1, 2] 1x HEPES is a solution of 25 mM HEPES and 150 mM NaCl adjusted to pH 7.6.

METHODS

Quantum dot (QD) synthesis. CdSe/4CdS/2ZnS/Zn^{2+} QDs were synthesized in a procedure adapted by Chern, *et al.,*[3] from Ghosh, *et al*.[4] CdSe cores were synthesized in a hot-injection method and shelled with CdS and ZnS in a successive ion layer and adsorption reaction (SILAR). Two and a half monolayers of ZnS were added with only the cation added in the last shell such that the QD surface was terminated with Zn^{2+}. The majority of the studies presented, including the DNA functionalization and most of the detailed characterization studies, were performed using these CdSe/CdS/ZnS core/shell/shell particles. InP/ZnS and InP/ZnSe/ZnS QDs produced using a previously published SILAR method were used to demonstrate generalizability to a cadmium-free system.[5] A one-pot synthesis of CdSe/CdS/ZnS alloyed shell particles was used to generate the green CdSe-based emitters for the energy transfer study described below.[6]

Polymer functionalization. The polymers were functionalized using a slightly modified version of a previously reported procedure.[2] In a typical experiment, for P1, 180 mg PIMA (poly(isobutylene-*alt*-maleic anhydride), 6,000 g/mol, 0.03 mmol, 1 equiv.) was dissolved in 3 mL

of anhydrous DMSO at 45°C. In parallel, 116 mg Me_3N^+-NH_2 (0.66 mmol, 22 equiv.), 73 mg histamine (0.66 mmol, 22 equiv.) and 193 µL triethylamine (1.39 mmol, 46 equiv.) were dissolved in 1.5 mL of anhydrous DMSO at 50°C. After complete dissolution of both solutions, the solution containing the amines was added with a syringe to the PIMA solution. The reaction was kept for 6h at 45°C. The polymer was precipitated in 1/1 ethyl acetate/diethyl ether, recovered in methanol, and reprecipitated in pure ethyl acetate. The polymer powder was dried under vacuum to obtain a white powder with 67% yield.

For P1-DBCO, the same protocol was used with a slightly different ratio of amines: 18 equivalents of histamine, 18 equivalents of Me_3N^+-NH_2, and 4 equivalents of DBCO were used per equivalent of PIMA.

For P2 and P2-DBCO, the Me_3N^+-NH_2 was replaced by sulfobetaine amine (Scheme S1) synthesized according to a previously published protocol.[1, 2]

For P3 and P3-DBCO, the Me_3N^+-NH_2 was replaced by a PEG-amine (550 g/mol). The polymers were precipitated twice in a 1/1 mixture of ethyl acetate/ether.

Polymer characterization. ^{1}H NMR were taken with an Agilent 500 MHz VNMRS spectrometer. The percentage of amine grafted was estimated by setting the isobutylene protons on the PIMA backbone at an integral of 6H (δ = 0.8-1 ppm); the other proton integrals were then estimated by comparison. For P1-P3 the number of imidazole groups is estimated by taking the average value of the 1H integrals at 7.2 ppm and at 8.5 ppm. For P1 and P1-DBCO, the number of Me_3N^+ is estimated by evaluating the 9H integral (δ = 3.1 ppm) of the 3 methyl groups on the quaternary amine. For P2 and P2-DBCO, the 4H peak (δ = 3.1 ppm) of the sulfobetaine is used. For P3 and P3-DBCO, the number of PEG chains is estimated by taking the 40H peak (δ = 3.6 ppm) of the CH_2-CH_2-O units of repetition. Since the 8 aromatic protons of DBCO (δ = 6.7-7.7 ppm) overlap the 1H of imidazole (δ = 7.2 ppm), the grafting efficiency of DBCO is calculated by subtracting the overall integral between δ = 6.7-7.7 ppm by the integral of 1H imidazole (δ = 8.5 ppm). Fourier transform infrared (FT-IR) spectra were taken on a Nicolet FT-IR with an attenuated total reflection (ATR) accessory to observe the disappearance of the C=O stretch band of the anhydride at 1770 cm^{-1} and the emergence of the C=O stretch of carboxylic acid and amide bonds at 1710 cm^{-1} and1650 cm^{-1}, respectively, indicating successful grafting.

Ligand exchange. In a typical experiment, 150 µL of QDs ([QD] = 4.8 µM, n = 0.7 nmol) were precipitated in 1 mL of ethanol and recovered in 1.5 mL chloroform. In parallel, 750 µL of P1 (10 mg/mL in DMSO, m = 7.5 mg) was dissolved in 750 µL of chloroform. The P1 solution was added to the QD dispersion and briskly stirred for 1 h. The ratio of DMSO/chloroform during ligand exchange was 25/75. After at least 1 h of stirring, 0.5 mL of 0.1 M NaOH was added, and the dispersion was quickly shaken by hand. The QDs transferred nicely to the aqueous phase (top). The water phase was extracted, centrifuged at 3,000 rpm for 1 min, and the supernatant filtered through a 100 nm PVDF syringe filter and buffer exchanged 3 times with 0.1 M $NaHCO_3$ using 100 kDa ultra-centrifugal filters (10,000 rpm, 2 min each cycle). QDs were recovered in 0.1 M $NaHCO_3$ at a final concentration of ~3 µM. The same protocol was used for P1-DBCO, P2, and P2-DBCO.

For ligand exchange with P3 and P3-DBCO, instead of a biphasic ligand transfer, the solubility of the PEG moieties requires that the QDs are first precipitated before reconstituting in water. The same protocol was used, but instead of adding NaOH directly to the QDs in DMSO/$CHCl_3$, ethyl acetate/ether (1/1) was added and the mixture centrifuged for 2 min at 10,000 rpm to obtain a

QD@P3(-DBCO) pellet. The samples were then recovered in 0.5 mL of 0.1 M NaOH before syringe filtering and buffer exchanging in the same manner as the other QD@P samples.

QD characterization. Photoluminescence (PL) spectra were measured on a HORIBA (Nanolog FL3-2iHR) fluorimeter. QDs were excited at 400 nm (slit-width = 5 nm) and emission was collected using a 300x500 grating centered around 600 nm (slit-width = 5 nm). The relative quantum yields of each of the samples was determined by plotting integrated emission as a function of absorption at excitation wavelength (488 nm) of 3-5 sample dilutions and comparing the resulting slope to that of Rhodamine 6G (R6G) in ethanol.[7] The quantum yield of R6G in ethanol is 94% and independent of concentration up to 20 µM when excited at 488 nm. Absorbance measurements were taken in a 1 cm cuvette on a Nanodrop 2000c spectrophotometer. The molar extinction coefficient of CdSe-based quantum dots was estimated by scaling their absorbance spectrum with previously reported empirical fits for CdSe extinction coefficients based on 1s peak position.[8]

The hydrodynamic diameter (D_h) of QD@P samples were recorded using Dynamic Light Scattering (DLS) on a Zetasizer Nano ZS90 (ZEN3690, Malvern Pananalytical).

The zeta potential of QD samples was measured on a Zetasizer Nano ZS90 (ZEN3690, Malvern Pananalytical). QDs tend to degrade during the measurements, so the reported zeta potentials were taken from 2 measurements of 20 scans.

TEM imaging was performed at Center for Nanoscale Systems (CNS), using a Jeol 2100 TEM, operating at 200 kV. TEM images were analyzed to determine QD nanocrystal size.

DNA conjugation. In a typical experiment, 0.02 nmol of QD@P (6.7 µL of ~3 µM QD@P) and 0.4 nmol of DNA-N_3 (~50 µM, DNA/QD = 20) were mixed with 0.1 M $NaHCO_3$ to a final volume of 70 µL. 70 µL of 2 M NaCl was added to obtain a final reaction solution comprising 0.14 µM QDs, 2.8 µM DNA-N_3, and 1 M NaCl. The mixture was left to react on an agitation plate for 4 days in the dark. Before purification, QD@P-DNA were analyzed on an agarose gel.

Gel mobility assay and imaging. QD@P and QD@P-DNA were analyzed using 1% agarose gels in 1x TBE (Tris-borate-EDTA) buffer or 1x TAE (Tris-acetate-EDTA). Typically, 10 µL of QDs at 0.1 µM was loaded on the gel per well. For QD@P-DNA, the gels were stained for at least 1 h with 4x Sybr Green. Gels were imaged in 3 different configurations. First, images were recorded on a Bio-Rad Imager ChemiDoc XRS equipped with a Universal Hood II Gel Doc System using the Image Lab software. An Azure Biosystems Sapphire imager (ex488/em518BP22) was used to exclude QD emission and capture only SybrGreen fluorescence for analysis. Lastly, we built our own system to verify and visualize colocalization of the green (DNA) and red (QD) bands. In this setup, gels were excited with a Thorlabs M455L3 (M00334196) 455 nm LED and two filters were used for capturing emission: a 350-600 nm band pass filter (Chroma Technology Corp BGG22-2mm) allowed both QD and DNA fluorescence through, while a 500 nm short pass filter was added to cut out QD emission and record DNA emission by itself.

DNA hybridization. For hybridization, QD@P-DNA were concentrated on 100 kDa ultra-centrifugal filters and recovered in duplex buffer (IDT Technologies). QD@P-DNA were hybridized by heating equimolar amounts of complementary strands and grafted DNA to 95°C for 2 minutes before cooling to 55°C by lowering the temperature 10°C every minute. Once 55°C was reached, the DNA was left to cool to room temperature by placing on a benchtop for 30-60 min.

Supplementary Figures and Tables

REACTION SCHEMES

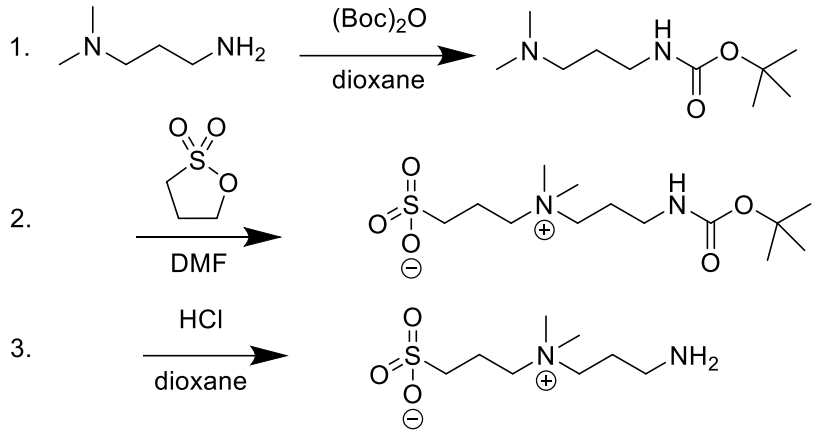

Scheme S1: Synthesis scheme for sulfobetaine-amine (from ref [1, 2]).

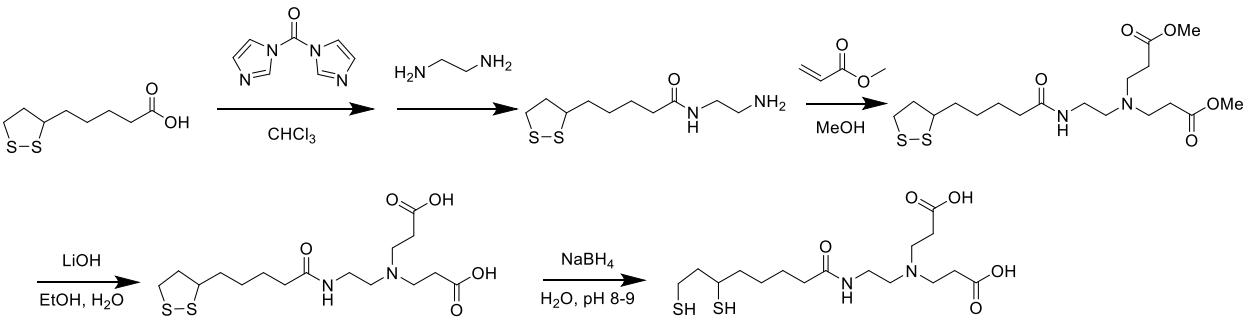

Scheme S2: Synthesis scheme for CL4 (from ref [9]).

POLYMER CHARACTERIZATION

For all polymers, the reaction yield was 70 ± 10%. The percentage of amines grafted is summarized in Table S1; the ^{1}H spectra upon which the grafting percentage calculations are based are provided in Figures S3-S8. FTIR spectra (Figure S9) exhibit the disappearance of the C=O stretch band of the anhydride at 1770 cm^{-1} and the emergence of the C=O stretch of carboxylic acid and amide bonds at 1710 cm^{-1} and1650 cm^{-1}, respectively, confirming successful grafting.

Table S1: Comparison of the polymers in this study including composition and estimation of resources required for their production, *i.e.*, an estimate of time (in days) and reagent cost.

Polymer	R	His[a] %	R[a] %	DBCO[a] %	n_{DBCO}[b]	$M_{n,th}$[a] g/mol	Reaction steps	Reaction time (days)	Price $/g[c]	Price $/mmol[c]	Ref[d]
P1	Me_3N^+	39	57	-	-	11,720	1	1	66	772	
P2	Zw	31	~30	-	-	10,070	4	7	38	477	2
P3	PEG	45	49	-	-	18,780	1	1	220	4013	10
P1-DBCO	Me_3N^+	38	48	9	3.6	12,040	1	1	390	4780	
P2-DBCO	Zw	41	41	9	3.6	12,490	4	7	325	4268	
P3-DBCO	PEG	36	56	10	4	21,020	1	1	368	6660	

[a] Percentage of amine moieties grafted on the PIMA polymer backbone, determined by ^{1}H NMR (with an error of ±5%) and estimation of the number average molecular weight by ^{1}H NMR. [b] Average number of DBCO per polymer chain estimated by ^{1}H NMR. [c] Price is calculated based on the price of reactants and solvents (Sigma Aldrich, USA); it does not consider the salary needed for the researcher's time spent or the standard lab equipment and consumables used in the procedure. [d] The polymers with no reference are presented for the first time in this work.

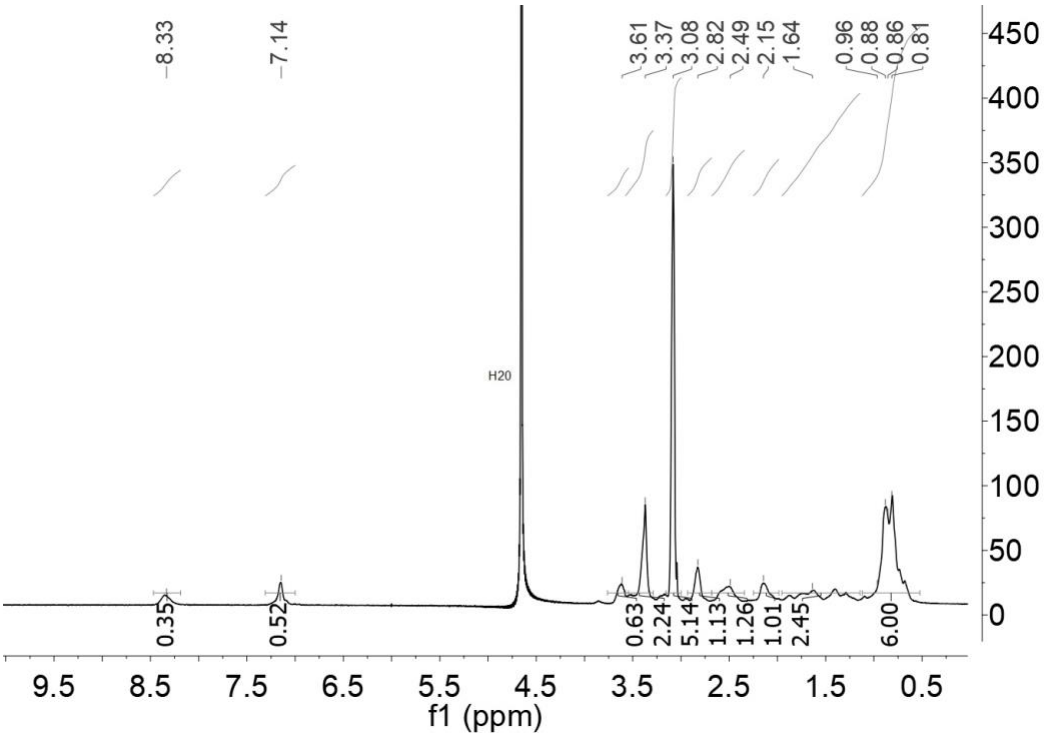

Figure S3: ^{1}H NMR of P1 in D_2O.

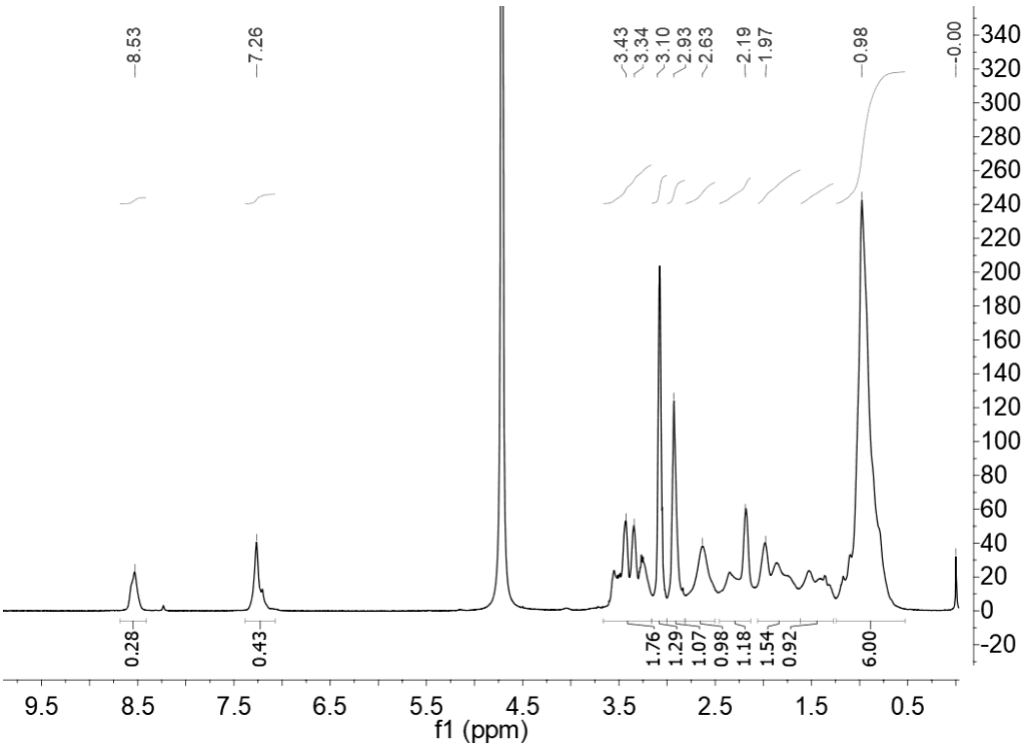

Figure S4: ^{1}H NMR spectra of P2 in D_2O.

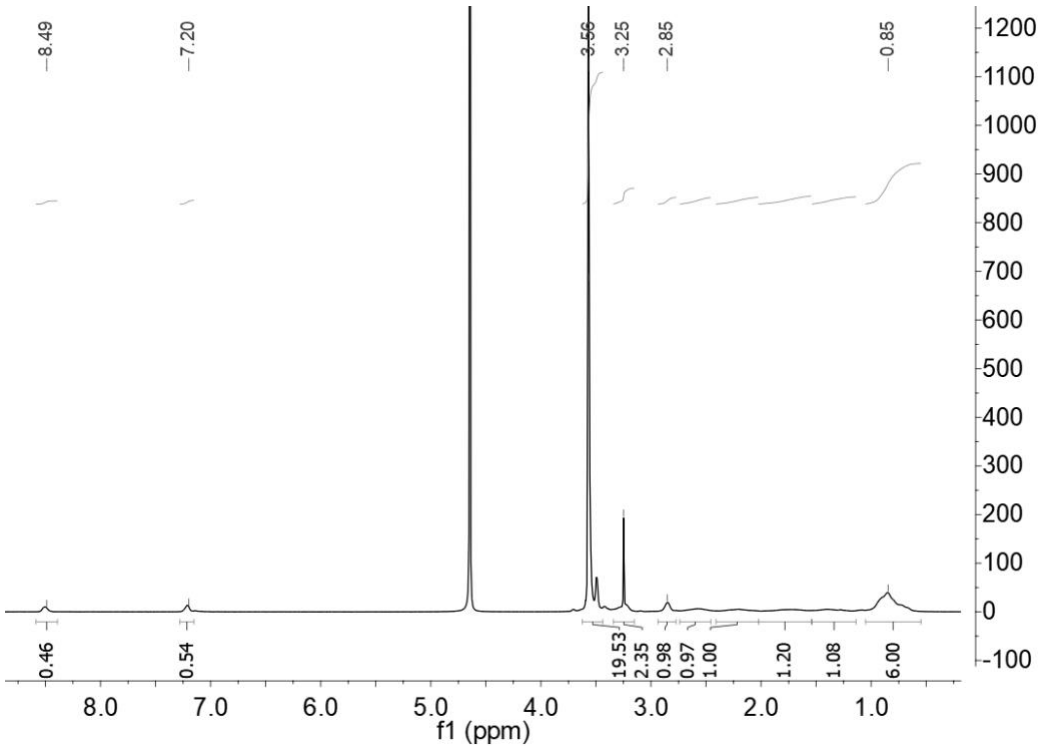

Figure S5: ^{1}H NMR spectra of P3 in D_2O.

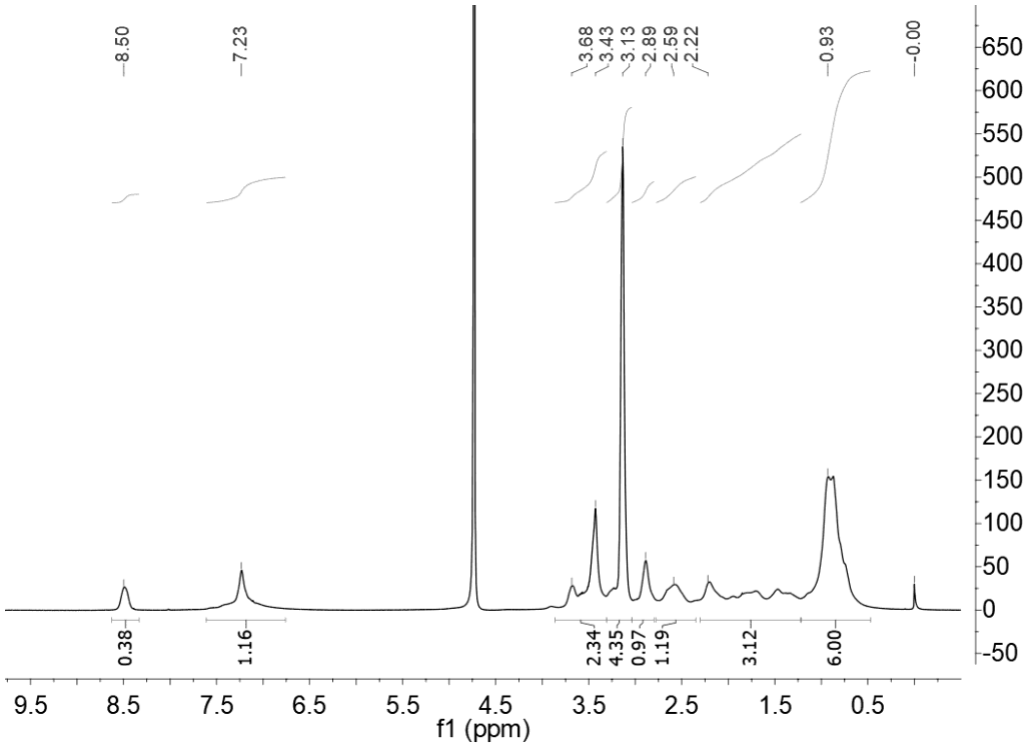

Figure S6: ^{1}H NMR spectra of P1-DBCO in D_2O.

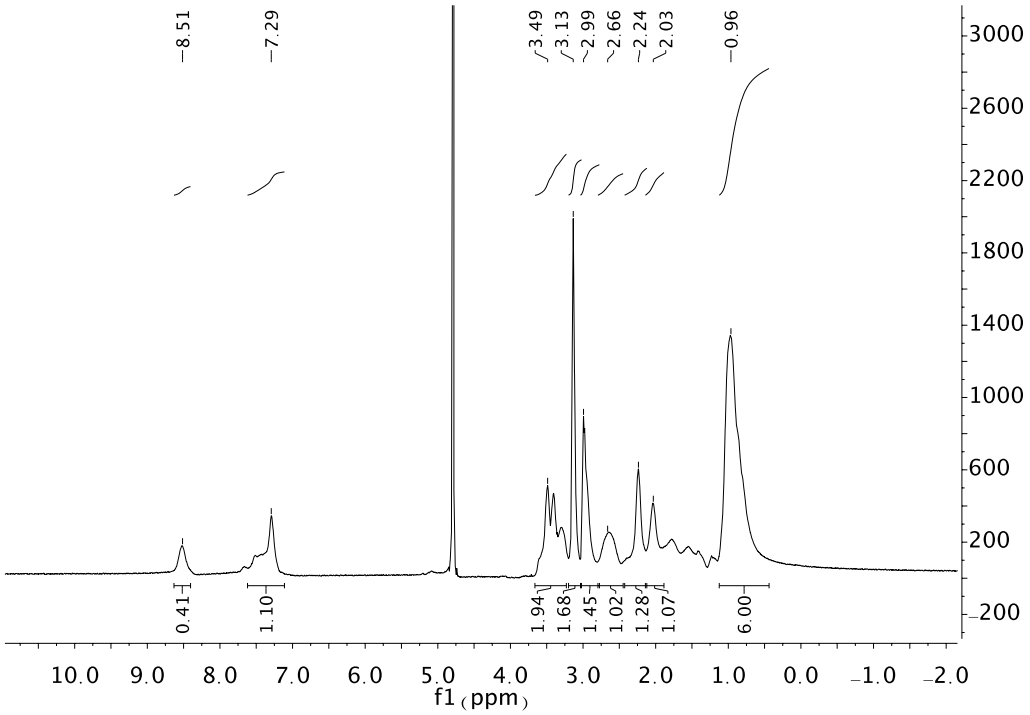

Figure S7: ^{1}H NMR spectra of P2-DBCO in D_2O.

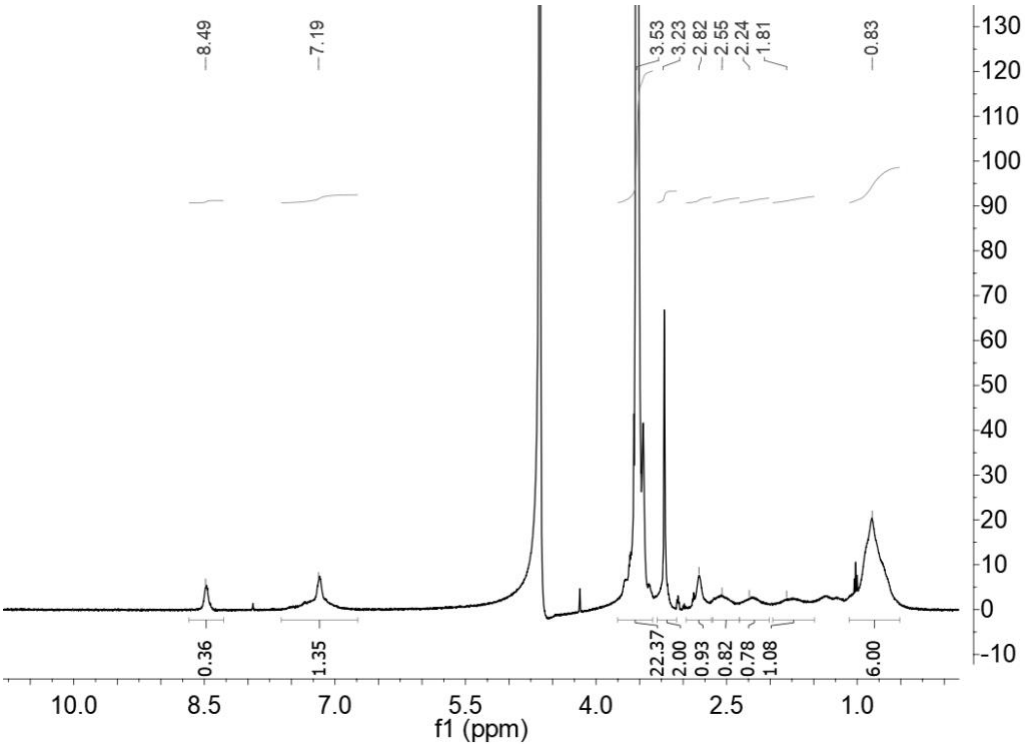

Figure S8: ^{1}H NMR spectra of P3-DBCO in D_2O.

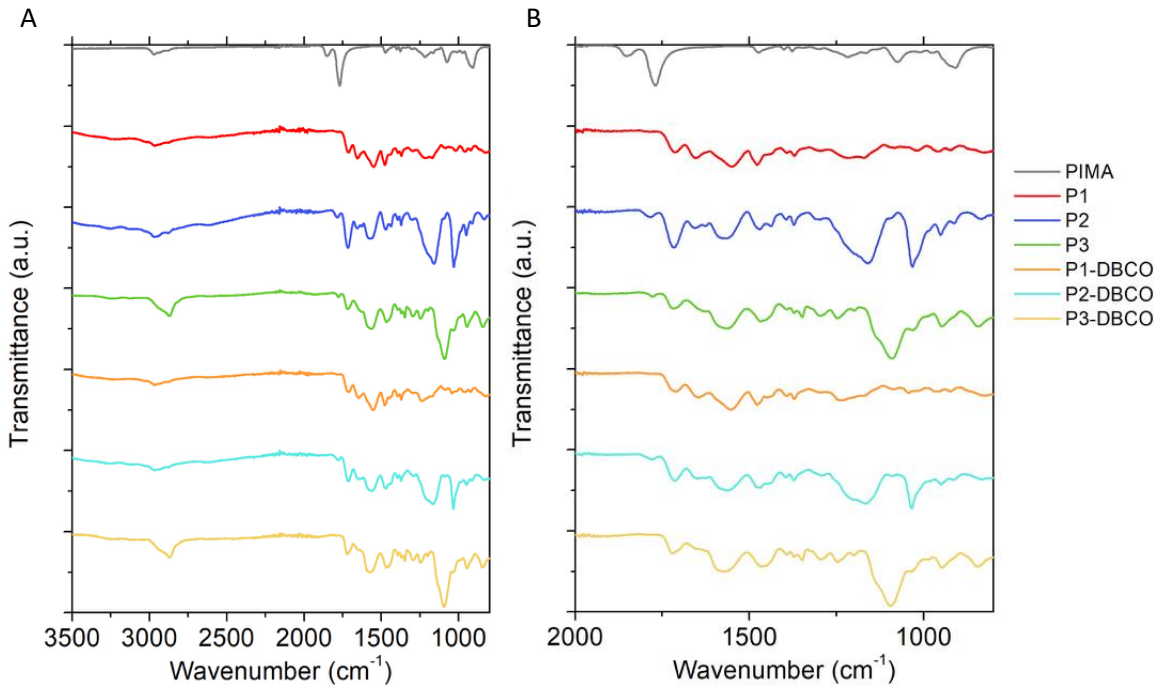

Figure S9: FTIR spectra of all polymer derivatives and comparison with the starting polymer PIMA. Data displayed **(A)** over full wavenumber range and **(B)** zoomed in to highlight features. Successful grafting of the amines results in a disappearance of the C=O stretch band of the anhydride at 1770 cm^{-1} and the presence of the C=O stretch of carboxylic acid and amide bonds at 1710 cm^{-1} and1650 cm^{-1}, respectively.

CHARACTERIZATION OF QD@P

The polymer-coated QDs were characterized by UV-vis absorption, photoluminescence spectroscopy, dynamic light scattering (DLS) and Zeta potential (ζ), and gel electrophoresis.

Table S2: Properties of QDs coated with different polymers analyzed at RT in 0.1x HEPES buffer (pH 7.6) for D_h and ζ and 1x HEPES for QY.

Polymer	D_h[a] (nm)	ζ[b] (mV)	QY[c] (%)
P1	10 ± 4	-12.7 ± 2.0	25
P2	12 ± 4	-36.0 ± 1.5	24
P3	9 ± 2	-18.1 ± 0.9	29
P1-DBCO	25 ± 7	-7.2 ± 0.1	41
P2-DBCO	16 ± 6	-53.5 ± 0.1	42
P3-DBCO	22 ± 7	-14.6 ± 0.5	42

[a] Hydrodynamic diameter (D_h) reported by number-weighted average ± standard deviation. [b] Zeta potential (ζ) reported as the average of two measurements ± standard deviation. [c] Quantum Yield (QY) are given with a ± 5% error.

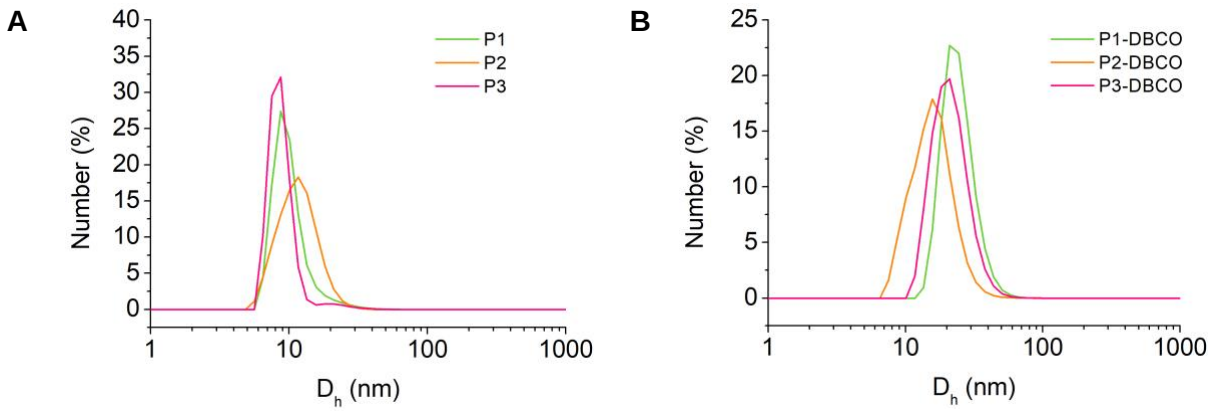

Figure S10: Hydrodynamic diameter distribution by **(A)** number of QD@P and **(B)** QD@P-DBCO measured by DLS at RT in 0.1x HEPES.

Gel mobility assay. QD@P samples were run on 1% agarose gels as described in the experimental section. Gels were adjusted to pH 6 or pH 8 and the results compared in order to determine the effects of pH on QD apparent charge.

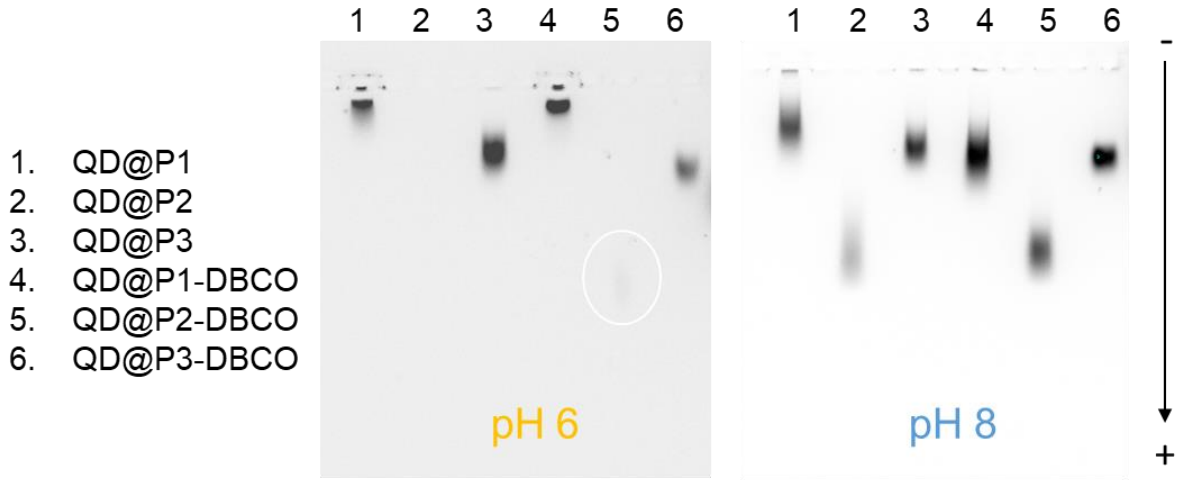

Figure S11: QD@P analyzed on 1% agarose gel in 1x TAE buffer adjusted to pH 6 or 8 (90V, 30 min). All samples are loaded at the same concentration, *i.e.,* 10 µL of QD at 0.5 µM in 0.1 M NaHCO3. On the left gel, the spot of QD@P2-DBCO is highlighted.

Stability data. Colloidal stability of QD@P solutions was evaluated by tracking changes in absorbance over a period of 8 days. A variety of conditions were tested: 1x HEPES at RT, 1x HEPES at 37ºC, 25 mM HEPES + 0 mM NaCl, 25 mM HEPES + 150 mM NaCl (*i.e.*, 1x HEPES), 25 mM HEPES + 300 mM NaCl, 0.15 M citrate-phosphate buffer (pH 5 at RT), 0.1 M Trizma buffer (pH 9 at RT).

For one storage condition (1x HEPES at room temperature) the colloidal stability of QDs coated with CL4 was also evaluated for comparison. QDs@CL4 showed decreased absorbance after 4 days indicating sedimentation of the samples. Their QYs were also much lower than the polymer coated QDs, but the phase exchange conditions for the QDs@CL4 were not optimized for ligand/QD ratio, amount of base used, and addition of Zn^{2+} ions, which have been previously shown to improve the QY of QDs cap-exchanged with thiol-based ligands.[11, 12]

All QD@P were stable in 25 mM HEPES (pH 7.6) with 0, 150, or 300 mM NaCl at RT as well as 1x HEPES (25 mM HEPES + 150 mM NaCl, pH 7.6) at 37ºC. At pH 5, QD@P1 aggregated almost immediately, indicating that the permanent positive charge of the quaternary ammonium is not sufficient to impart colloidal stability once the carboxylic acids are protonated. QD@P2 and QD@P3 also showed signs of aggregation at pH 5, but not to the extent exhibited by QD@P1. Interestingly, their DBCO counterparts (QD@P2-DBCO and QD@P3-DBCO) were stable at pH 5, and QD@P1-DBCO exhibited less aggregation than QD@P1 (Figure S12).

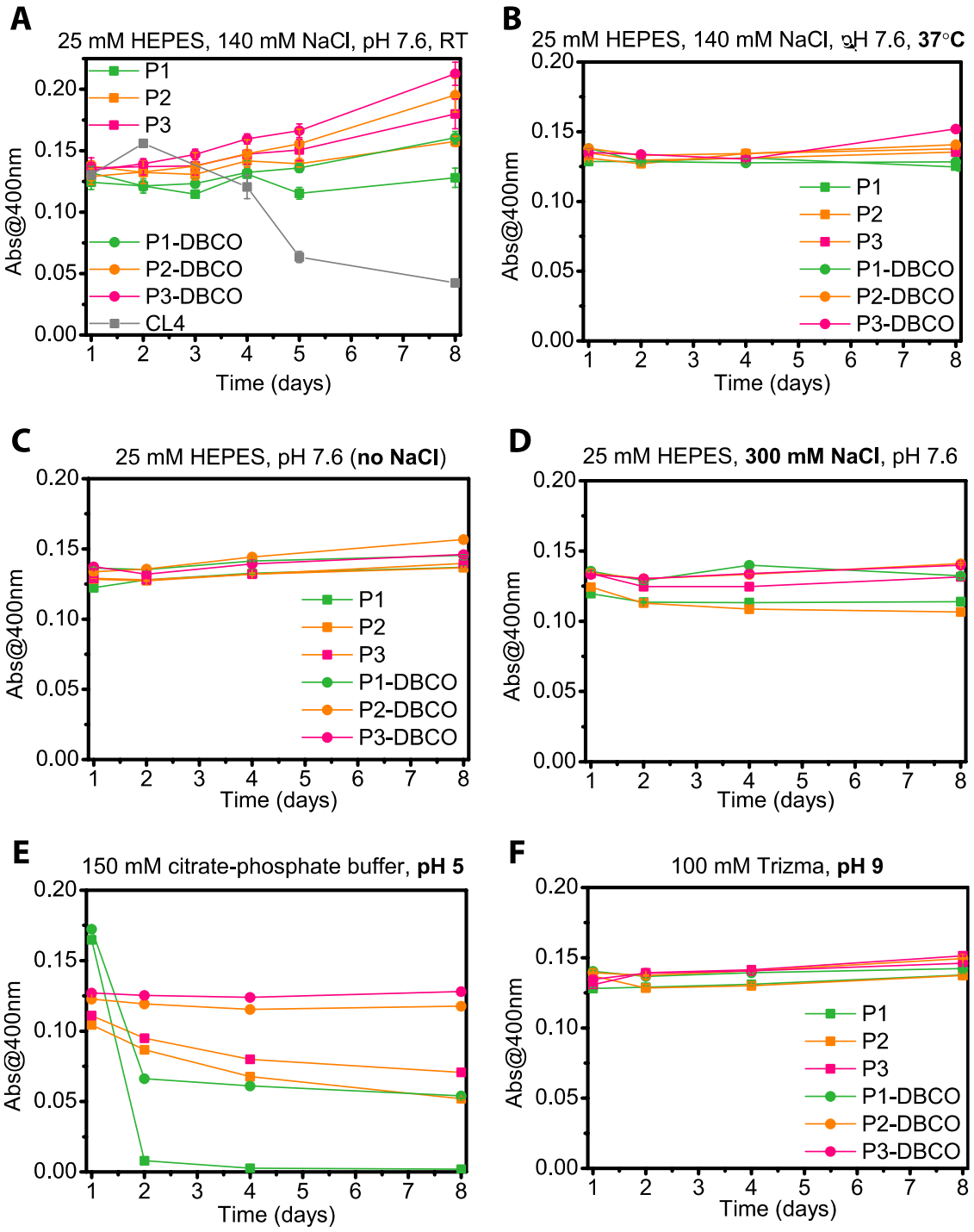

Figure S12: Colloidal stability of QD@P polymers observed through absorbance at 400 nm over time. (A) 1x HEPES (25 mM HEPES, 150 mM NaCl, pH 7.6) at RT. **(B)** 1x HEPES at 37°C. **(C)** 25mM HEPES, 0 mM NaCl, pH 7.6, RT. **(D)** 25 mM HEPES, 300 mM NaCl, pH 7.6, RT. **(E)** 150 mM Citrate-Phosphate buffer (100 mM Na_2HPO_4 + 50 mM citric acid), pH 5, RT. **(F)** 100 mM Trizma buffer, pH 9, RT.

FRET and self-assembly. A Förster resonance energy transfer (FRET) assay was used to verify histidine tag-mediated self-assembly as well as to demonstrate the potential for using QD@P1s as FRET donors in biosensing applications. A green emitting QD donor (QD_{505}) was paired with his-tagged fluorescent protein tdTomato (acceptor). If the donor and acceptor are brought into close proximity (2 – 10 nm), energy transfer will result in a quenching of the QD donor emission and sensitized acceptor emission. FRET assays were performed in triplicate similar to previously described reports.[3] The QD concentration was fixed at 50 nM for every experiment, while the concentration of his-tagged tdTomato was increased to increase acceptor to donor ratio. All experiments showed FRET sensitized acceptor emission (Figure S11) indicating that histidine based self-assembly is not hindered by the polymer.

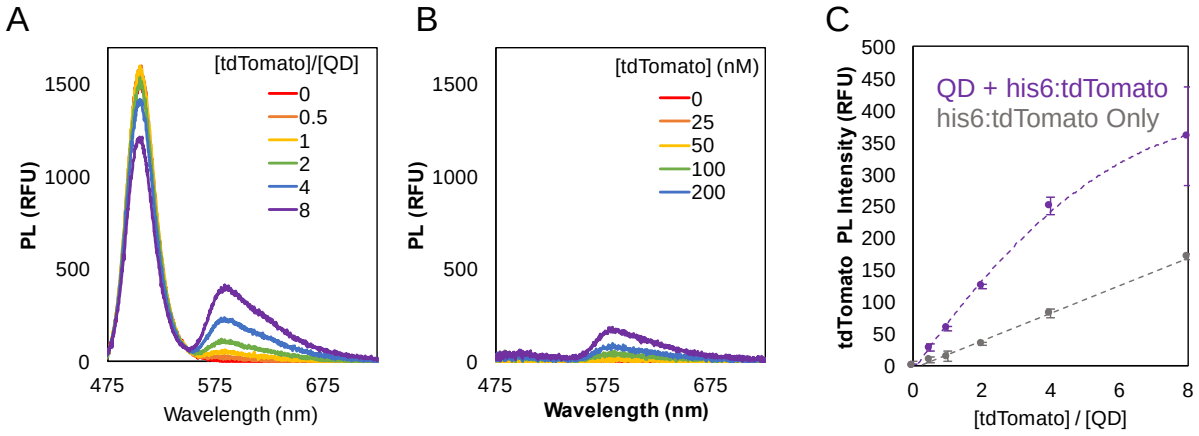

Figure S13: (**A**) Raw PL spectra from the FRET assays performed using QD_{505}@P1. (**B**) Direct acceptor excitation signal from tdTomato-only wells. (**C**) tdTomato fluorescence intensity with and without the presence of the QD_{505} donor showing enhanced emission from tdTomato as a FRET acceptor.

Overlap integral and Förster distance were calculated using Eqns. 1 & 2, respectively. Quantum yields were taken using an integrating sphere with excitation at 400 nm. Experimentally determined FRET efficiencies and donor-acceptor separation distance (r_{exp}) were calculated using Eqn. 3.

FRET Equations:

$$J(\lambda) = \int \frac{f_D(\lambda)}{\int f_D(\lambda) d\lambda} \varepsilon_A(\lambda) \lambda^4 d\lambda \qquad \text{Eqn. 1}$$

$$R_0(\text{nm}) = 0.0218 \left[\frac{\kappa^2 \Phi_D}{n^4} \left(\frac{J(\lambda)}{\text{M}^{-1}\,\text{cm}^{-1}\,\text{nm}^4} \right) \right]^{1/6} \qquad \text{Eqn. 2}$$

$$E_{FRET} = 1 - \frac{F_{DA}}{F_D} = \frac{n{R_0}^6}{n{R_0}^6 + r^6} \qquad \text{Eqn. 3}$$

where $f_D(\lambda)$ is the fluorescence spectrum of the donor (which is normalized to 1 by dividing by its total area), and $\varepsilon_A(\lambda)$ is the molar absorptivity of the acceptor, all scaled to wavelength, λ; $J(\lambda)$

has units of $\mathrm{M}^{-1}\,\mathrm{cm}^{-1}\,\mathrm{nm}^4$. κ^2 is the dipole orientation factor between the donor and acceptor, Φ_D is the quantum yield of the donor, and n is the solvent refractive index. The dipole orientation factor was assumed to be 2/3, as it is the value for an isotropic (*i.e.,* randomly oriented) system.

Table S3: FRET parameters of interest.

FRET: Donor & Acceptor Characteristics			
QD_{505}		tdTomato	
PL_{max} (nm)	505	Ex_{max} (nm)	554
r_{TEM} (nm)	5.0 ± 0.5	ε_{554} (M^{-1} cm^{-1})	138,000
J (M^{-1} cm^{-1} nm^4): 4.47×10^{15}			
FRET: Experimental Data			
Donor	QY (%)	E_{max} (%, n = 8)	R_0 (nm)	r_{exp} (nm)
QD505@P1	19 ± 1	20.5	5.01	8.87

DBCO handles per polymer. The number of DBCO units per QD is estimated by absorption using ε_{DBCO}(309 nm) = 12,000 $M^{-1}cm^{-1}$ and ε_{QD}(400nm) = 2.6×10^6 $M^{-1}cm^{-1}$ (Figure S12 and Table S4). The absorption spectrum of QD@P is subtracted from the absorption spectra of QD@P-DBCO to obtain the absorption of P-DBCO by itself.

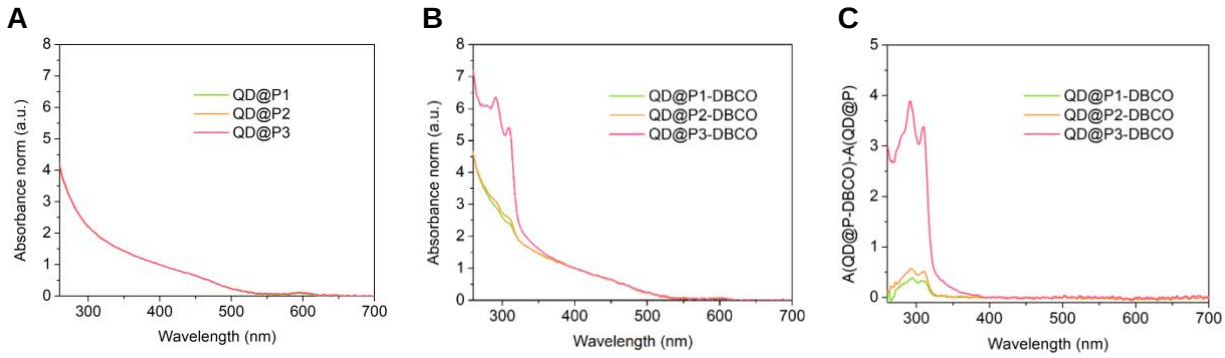

Figure S14: Determination of DBCO presence using UV-Vis spectrophotometry. (A) Absorption spectra of QDs@P. **(B)** Absorption spectra of QDs@P-DBCO. **(C)** Absorbance spectra of QDs@P subtracted from QDs@P-DBCO to obtain the contribution from DBCO.

Table S4: Number of DBCO per polymer determined by ^{1}H NMR and number of P-DBCO per QD determined by absorption. Numbers obtained from QD@P purified by precipitation after ligand exchange are indicated with *. All other numbers reported used a biphasic ligand exchange.

	P1-DBCO	P2-DBCO	P3-DBCO
DBCO/P	3.6	3.6	4
P/QD exp 1	14	33	80*
P/QD exp 2	16	24	108*
P/QD exp 3	15*	32*	97*
average	15	30	95
stedv	1	4	11
DBCO/QD	55	107	381

DNA-QD GRAFTING

Table S5: DNA sequences used in this study.

Name	Abbreviation	Sequence 5'→ 3'
DNA-azide	DNA-N_3	N_3-T TTT CGT GTC CCT CGC TCG GTT TC
cDNA-azide	cDNA	GA AAC CGA GCG AGG GAC ACG
cDNA-azide-biotin	cDNA-bt	Biotin-GA AAC CGA GCG AGG GAC ACG

DBCO/azide reaction ratios. The DNA grafting scheme relies on DBCO-azide click coupling. The DBCO/DNA-N_3 ratios are given here for reference (Table S6).

Table S6: Grafting of DNA-N_3 on QD@P-DBCO: molar ratio of DBCO per quantum dots and DNA-N_3 per Quantum dots or DBCO on the QD.

Exp	DBCO / QD	DNA-N_3 / QD	DBCO / DNA-N_3
QD@P1-DBCO@DNA-a	55	20 (control, DNA-NH_2)	2.8 (control)
QD@P1-DBCO@DNA-b	55	50	1.1
QD@P1-DBCO@DNA-c	55	20	2.8
QD@P2-DBCO@DNA-a	107	20 (control, DNA-NH_2)	5.4 (control)
QD@P2-DBCO@DNA-b	107	50	2.1
QD@P2-DBCO@DNA-c	107	20	5.4
QD@P3-DBCO@DNA-a	381	20 (control, DNA-NH_2)	19.1 (control)
QD@P3-DBCO@DNA-b	381	50	7.6
QD@P3-DBCO@DNA-c	381	20	19.1

Grafting efficiency. DNA grafting efficiency was evaluated *via* agarose gel. Visual inspection of SybrGreen stained gels are helpful in verifying that DNA is grafted to the QD (green colocalized with red). Additionally, the absence of fluorescence in line with the free DNA seen for the control reactions (a) indicates high grafting efficiency.

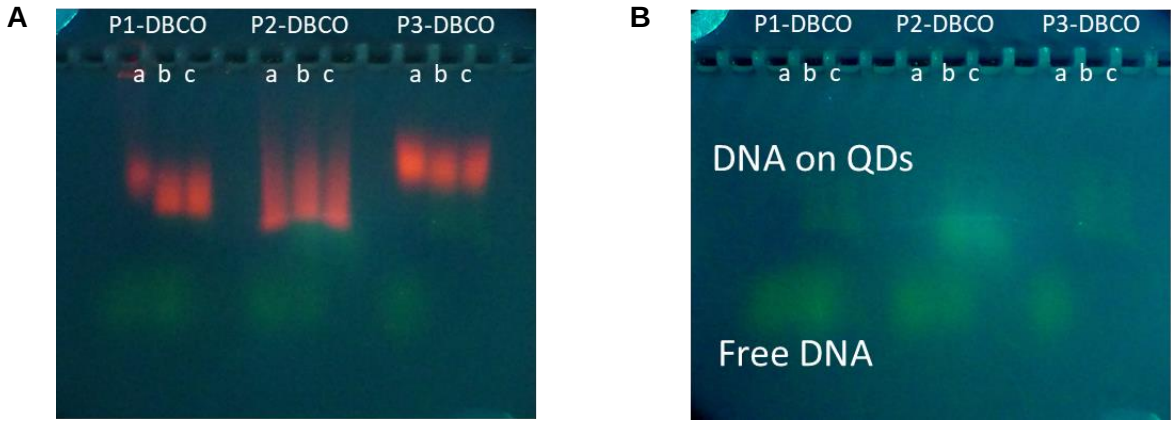

Figure S15: Image of 1% Agarose gel in 1X TBE buffer stained with SybrGreen taken with a camera on the home-made setup. All QD@P-DBCO are loaded at the same concentration with the same reaction conditions. Labels correspond to conditions listed in Table SI 6. (A) Imaging with bandpass emission filter enables visualization of both QD and DNA fluorescence. (B) Imaging with shortpass + bandpass filter exhibits only DNA fluorescence.

Image analysis. Quantitative analysis of grafting efficiency was obtained by analyzing images collected with an Azure Biosystems Sapphire imager as previously described. The percentage of free DNA was determined on image excluding the QD fluorescence (Figure S16).

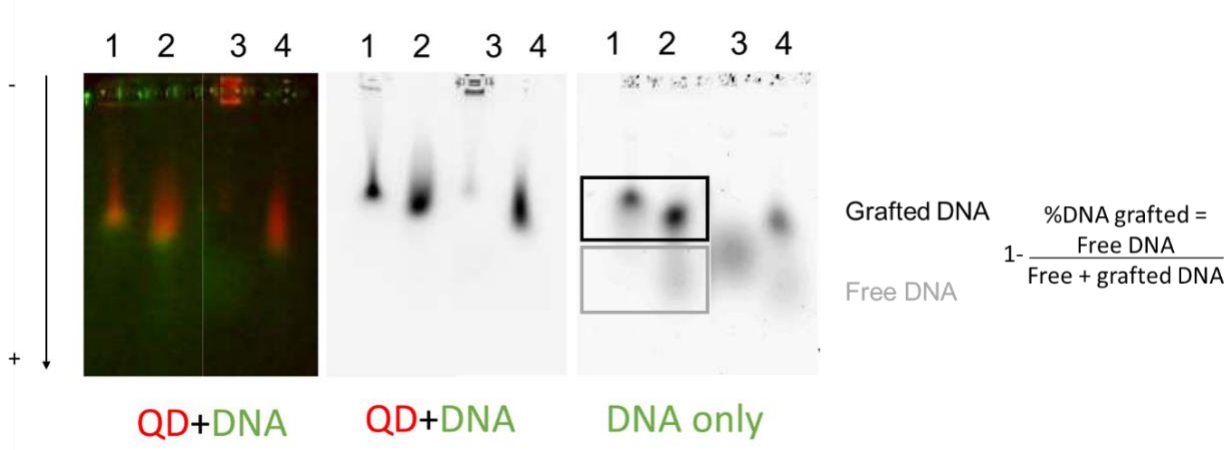

Figure S16: Image of 1% agarose gel in 1X TAE buffer showing the efficient grafting of DNA onto QD surface. Grafting conditions: (**1**) *high salt:* QD@P1-DBCO + 20x DNA-N_3 in 0.1 M $NaHCO_3$, 1 M NaCl; (**2**) *low salt:* QD@P1-DBCO + 20x DNA-N_3 in 1x HEPES; (**3**) *high salt negative control (no azide on DNA):* QD@P1-DBCO + 20x DNA-NH_2 in 0.1 M $NaHCO_3$, 1 M NaCl; (**4**) *no salt:* QD@P1-DBCO + 20x DNA-N_3 in 0.1 M $NaHCO_3$. **Left**: picture with a camera equipped with a 500 nm shortpass filter; **middle**: Bio-Rad imager; **right**: Azure Imager.

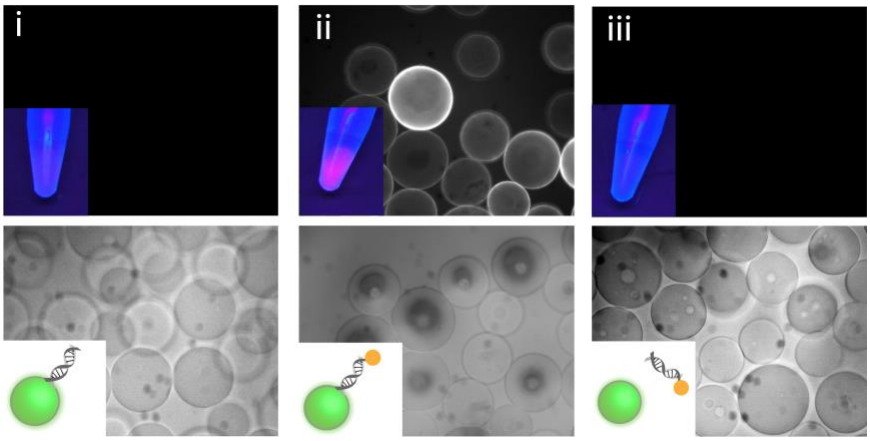

Figure S17: Microscopy of streptavidin-coated agarose beads labeled with QDs biotinylated through DNA grafting and hybridization. (Top) Fluorescent and **(bottom)** bright field microscope images of the SA beads incubated with **(i)** QD-dsDNA (no biotin), **(ii)** QD-dsDNA-bt, and **(iii)** QDs mixed with dsDNA-bt. Insets show pictures of each sample under UV-illumination.

Quantification of Hybridization. The amount of ssDNA available for hybridization was quantified by UV-Vis absorption before and after hybridization. Samples starting with ~20 ssDNA/QD were hybridized as described above. The samples were washed 3x on 50 kDa centrifugal filtration devices both before and after hybridization to rid the solutions of any unreacted, free DNA from both the SPAAC and hybridization reactions. Absorbance spectra were analyzed to distinguish absorbance from DNA vs. QDs (see DBCO quantification methods) before quantifying DNA concentration by absorbance at 260 nm. The molar extinction coefficient for the dsDNA (350,080 M^{-1} cm^{-1}) was estimated by summing the molar extinction coefficients of the two complement strands given by the vendor and considering the hypochromicity effect[13] as given by Equation 4, where f_{AT} and f_{GC} are fractions of AT and GC base pairs, respectively. The ssDNA/QD and dsDNA/QD ratios calculated through this analysis are given in Table S7 and show that all QD@Ps exhibited greater than 50% hybridization efficiency. The highest percentage of ssDNA was hybridized when using QDs@P3 (79%) while the lowest percentage (54%) was seen when using QDs@P2.

$$\varepsilon_{dsDNA} = (1 - 0.287 f_{AT} + 0.059 f_{GC})(\varepsilon_{s1} + \varepsilon_{s2}) \qquad \text{Eqn. 1}$$

Table S7: Quantification of Hybridization.

Polymer used	ssDNA / QD	dsDNA / QD	% hybridized
P1-DBCO	18	11	61
P2-DBCO	13	7	54
P3-DBCO	19	15	79

REFERENCES

1. G. Kim, C. E. Yoo, M. Kim, H. J. Kang, D. Park, M. Lee and N. Huh, *Bioconjugate Chem.*, 2012, **23**, 2114-2120.
2. W. Wang, X. Ji, A. Kapur, C. Zhang and H. Mattoussi, *JACS*, 2015, **137**, 14158-14172.
3. M. Chern, T. T. Nguyen, A. H. Mahler and A. M. Dennis, *Nanoscale*, 2017, **9**, 16446-16458.
4. Y. Ghosh, B. D. Mangum, J. L. Casson, D. J. Williams, H. Htoon and J. A. Hollingsworth, *JACS*, 2012, **134**, 9634-9643.
5. R. Toufanian, A. Piryatinski, A. H. Mahler, R. Iyer, J. A. Hollingsworth and A. M. Dennis, *Front Chem*, 2018, **6**.
6. W. K. Bae, K. Char, H. Hur and S. Lee, *Chem. Mater.*, 2008, **20**, 531-539.
7. M. Fischer and J. Georges, *Chem. Phys. Lett.*, 1996, **260**, 115-118.
8. W. W. Yu, L. Qu, W. Guo and X. Peng, *Chem. Mater.*, 2003, **15**, 2854-2860.
9. K. Susumu, E. Oh, J. B. Delehanty, J. B. Blanco-Canosa, B. J. Johnson, V. Jain, W. J. Hervey, W. R. Algar, K. Boeneman, P. E. Dawson and I. L. Medintz, *JACS*, 2011, **133**, 9480-9496.
10. W. Wang, A. Kapur, X. Ji, M. Safi, G. Palui, V. Palomo, P. E. Dawson and H. Mattoussi, *JACS*, 2015, **137**, 5438-5451.
11. D. Liu and P. T. Snee, *ACS Nano*, 2011, **5**, 546-550.
12. W. Wang, Y. Guo, C. Tiede, S. Chen, M. Kopytynski, Y. Kong, A. Kulak, D. Tomlinson, R. Chen, M. McPherson and D. Zhou, *ACS Appl. Mater. Interfaces*, 2017, **9**, 15232-15244.
13. A. V. Tataurov, Y. You and R. Owczarzy, *Biophys. Chem.*, 2008, **133**, 66-70.